IWARA 2018

Experimental design and progress for testing Lorentz symmetry in gravity

ChengGang Shao

Center for Gravitational Experiment (CGE),

Huazhong University of Science and Technology (HUST),

Wuhan, China

2018.09.13 Peru 2018

Outline

- The background of LV in gravity
- ISL experiments in HUST
- Experiments test for LV in short-range gravity
- New experimental design for LV

I. Background of LV in gravity

Gravitational phenomena ←

GR ← Einstein Equivalence Principle (three logical parts):

Weak equivalence principle (WEP)

Local Lorentz invariance (LLI)

Local Position invariance (LPI)

- Lorentz violation in gravity

Lorentz violation ---- Described by the presence of background general tenser fields in spacetime ($s_{\mu\nu}$, $k_{\mu\nu\kappa\lambda}, \cdots$)

The topic :

Recent progress on probing LV in gravity at HUST

Background of LV in gravity

General framework: Standard-Model Extension (SME)

(developed by Kostelecky and collaborators)

Lagrangian of LV in **gravity**

$$L_{\mathrm{LV}} = \frac{\sqrt{g}}{16\pi G}\left(L_{\mathrm{LV}}^{(4)} + L_{\mathrm{LV}}^{(5)} + L_{\mathrm{LV}}^{(6)} + \cdots\right)$$

Bailey, PRD91,022006(2015)

a series involving operators of increasing mass dimension d

$L_{\mathrm{LV}}^{(4)}$ $\leftarrow$ **Tested by interaction between Earth and a small test body.**

$L_{\mathrm{LV}}^{(5)}$ has no effect on nonrelativistic gravity

$L_{\mathrm{LV}}^{(6)}$ $\leftarrow$ **Tested in short-range gravity.**

Minimal SME(mSME d=4)

The minimal term with $d = 4$

$$L_{\mathrm{LV}}^{(4)} = (k^{(4)})_{\alpha\beta\gamma\delta} R^{\alpha\beta\gamma\delta}$$

The dimensionless coefficient

trace

$$-uR + s^{\mu\nu} R_{\mu\nu} + t^{\kappa\lambda\mu\nu} R_{\kappa\lambda\mu\nu}$$

$$V(r) = -G \frac{m_1 m_2}{|\vec{x}_1 - \vec{x}_2|} \left[1 + \frac{1}{2} \hat{x}^j \hat{x}^k \bar{s}_{jk} \right]$$

- Atom-interferometer
- Lunar laser ranging
- Pulsar-timing observations

9 independent components $\bar{s}^{\mu\nu} \sim 10^{-10}$

Laboratory experiments: To measure the acceleration of a free body

Due to the Earth's orbit and rotation

the local acceleration for LV $\dfrac{g_{\mathrm{LV}}}{g} \propto \sum_m C_m \cos \omega_m t + D_m \sin \omega_m t$

Six frequencies $\omega_m = (2\omega_\oplus, \omega_\oplus, 2\omega_\oplus + \Omega,\ 2\omega_\oplus - \Omega, \omega_\oplus + \Omega, \omega_\oplus - \Omega)$

C.G.Shao. etal, PRD97,024019 (2018)

Non-minimal term with $d = 6$

LV in short-range gravity. Bailey, PRD91,022006(2015)

Lagrangian includes quadratic couplings of Riemann curvature

$$L_{\mathrm{LV}}^{(6)} = \frac{1}{2}(k_1^{(6)})_{\alpha\beta\gamma\delta\kappa\lambda}\{D^\kappa, D^\lambda\}R^{\alpha\beta\gamma\delta} + (k_2^{(6)})_{\alpha\beta\gamma\delta\kappa\lambda\mu\nu} R^{\alpha\beta\gamma\delta} R^{\kappa\lambda\mu\nu}$$

In nonrelativistic limits

LV is described by the effective coefficients $(\bar{k}_{eff})_{jklm}$

Totally symmetric indices

Modified Possion equation $\nabla^2 U + 4\pi G\rho(\vec{r}) + (\bar{k}_{eff})_{jklm}\partial_j\partial_k\partial_l\partial_m U = 0$

In the case of two point masses $V(r) = -G\dfrac{m_1 m_2}{r}\left[1 + \dfrac{\bar{k}(\hat{r})}{r^2}\right]$

Potential between two point masses

$$V_{\mathrm{LV}}(\vec{r}) = -Gm_1m_2\frac{\bar{k}(\hat{r})}{r^3} \quad r = |\vec{x}_1 - \vec{x}_2|$$

anisotropic combination of coefficients $(\bar{k}_{eff})_{ijkl}$,

function of $\hat{r}$ direction

Bailey, PRD91,022006(2015)

$$\bar{k}(\hat{r}) = \frac{3}{2}(\bar{k}_{eff})_{iijj} - 9(\bar{k}_{eff})_{ijkk}\hat{r}^i\hat{r}^j + \frac{15}{2}(\bar{k}_{eff})_{ijkl}\hat{r}^i\hat{r}^j\hat{r}^k\hat{r}^l$$

Compare to usual Yukawa potential $V_{Yuk}(r) = -Gm_1m_2\frac{\alpha e^{-r/\lambda}}{r}$

Distinctive feature of LV : anisotropic cubic potential

depends on sidereal time in lab frame

Tests in short-range gravity

- constrain Yukawa parameter (α, λ)
- constrain Lorentz violation $(\bar{k}_{eff})_{jklm}$

Application

$$V(r) = -G\frac{m_1 m_2}{\left|\vec{x}_1 - \vec{x}_2\right|}\left(1 + \frac{1}{2}\hat{x}^{\hat{j}}\hat{x}^{\hat{k}}\bar{s}^{\hat{j}\hat{k}}\right)$$

Gravitational experiments in HUST

- **Measurement of G、g(tidal)**
- **Test of weak equivalence principle (WEP)**
- **Test of Newtonian inverse square law (ISL)**

Yukawa-type potential :

$$V(r) = -G\frac{m_1 m_2}{r}\left(1 + \alpha e^{-r/\lambda}\right)$$

Lorentz violation potential :

$$V(r) = -G\frac{m_1 m_2}{r}\left(1 + \frac{\bar{k}(\hat{r})}{r^2}\right)$$

II. ISL experiments in HUST

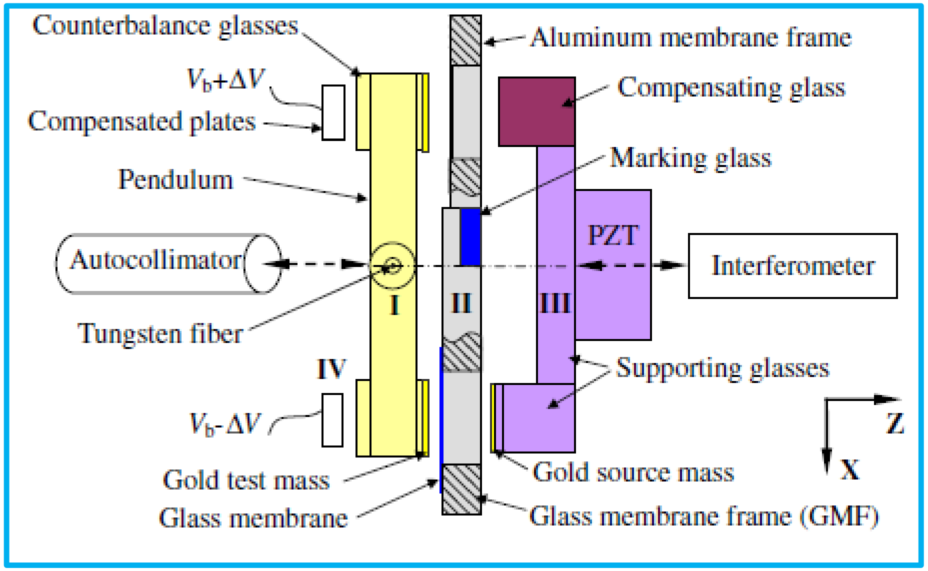

Basic feature: I-shaped pendulum, gold

Source mass platform: facing the pendulum, I-shaped structure

The separation was modulated by driving a motor translation stage

Ranging from176 to 341 μm

ISL Experiment, **HUST-2007**

PRL 98,201101(2007)

$2.1*10^{-16}$Nm

Our first result is not very good.

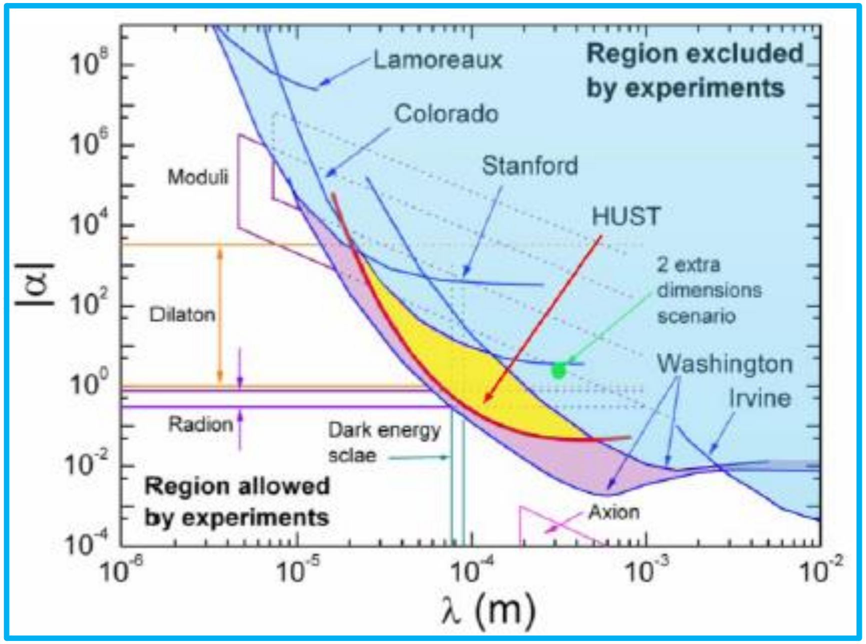

ISL experiment --HUST-2011

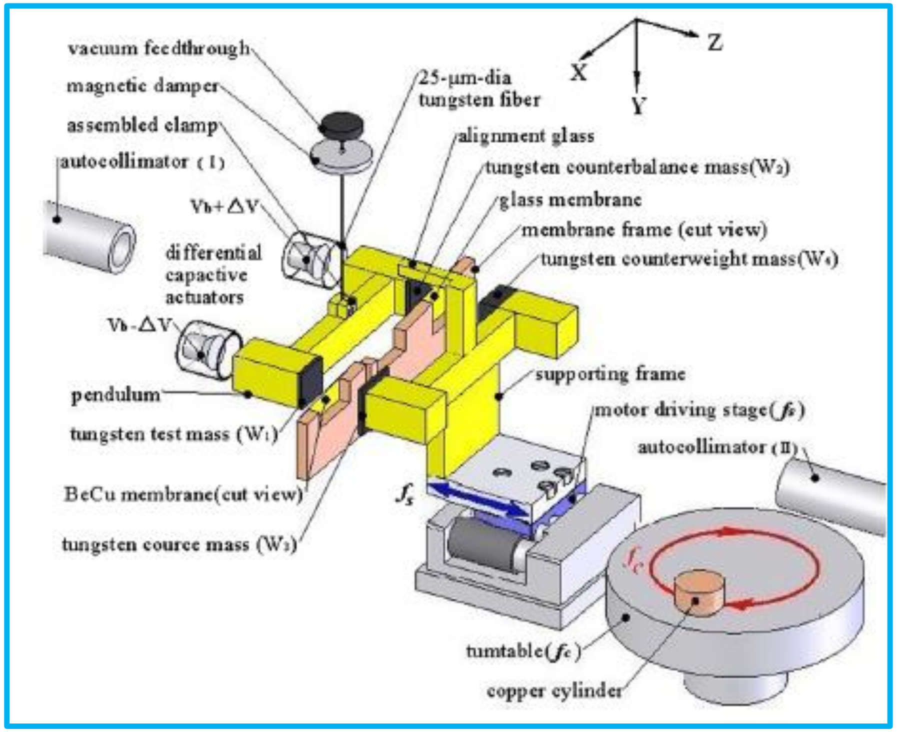

The material of test and source masses: Tungsten instead of gold

The separation was modulated by driving a motor translation stage

Ranging from 0.4 to 1.0 mm

ISL Experiment, HUST-2011

PRL 108,081101(2012)

$1.59*10^{-16}$Nm

At the length scale of several millimeters, we improve the previous bounds by up to a factor of 8.

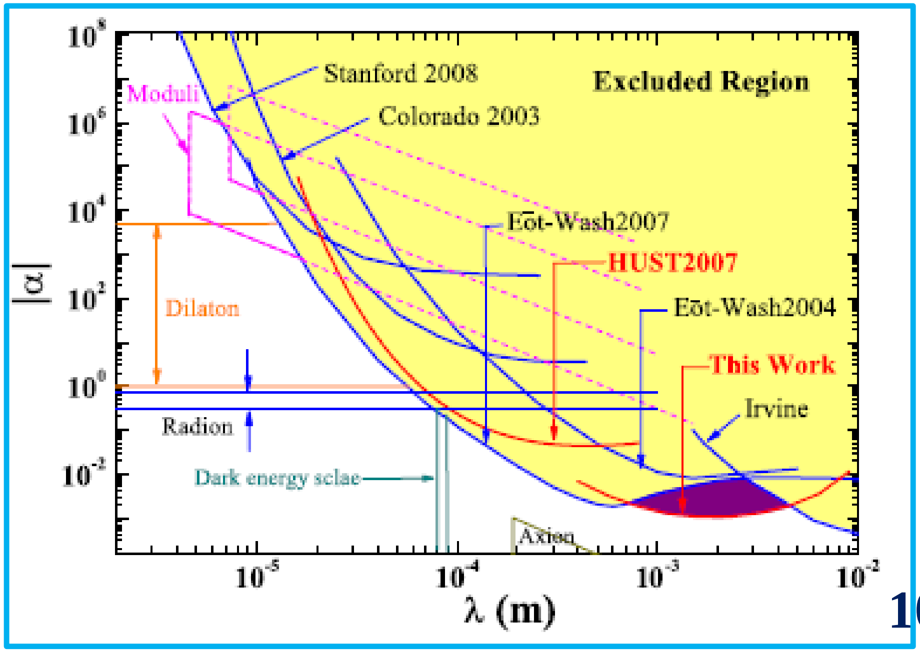

ISL experiment --HUST-2015

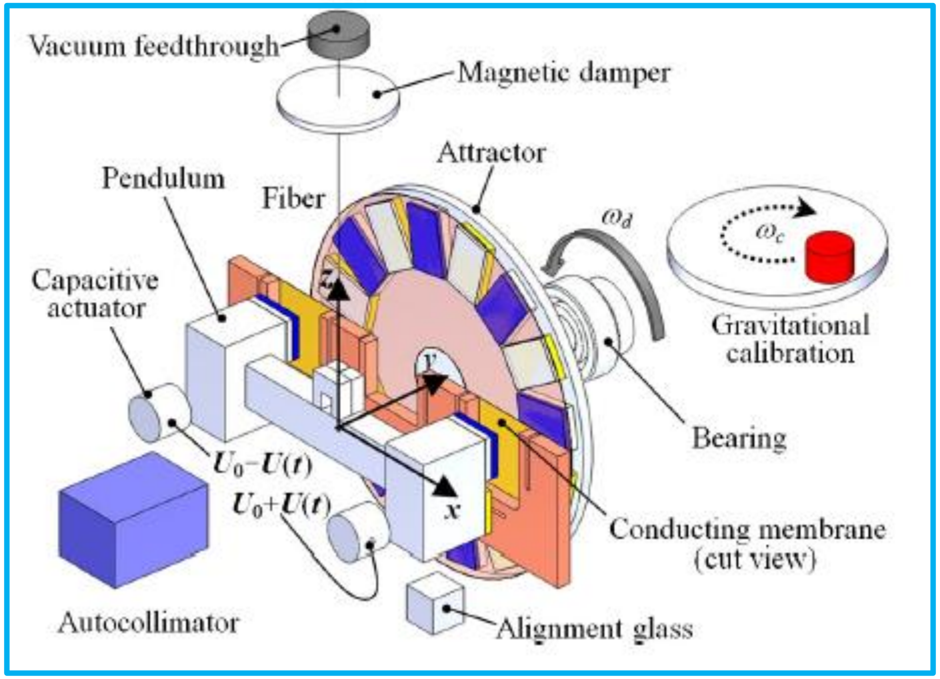

I-shaped pendulum, tungsten

Source mass platform: facing the pendulum, glass disk structure

a rotating eightfold symmetric attractor

separation: 0.295 mm

ISL Experiment, HUST-2015

PRL 116, 131101 (2016)

$2.0*10^{-17}$Nm

This experiment improves the previous bounds by up to a factor of 2 at the length scale $\lambda \approx 160\ \mu$m.

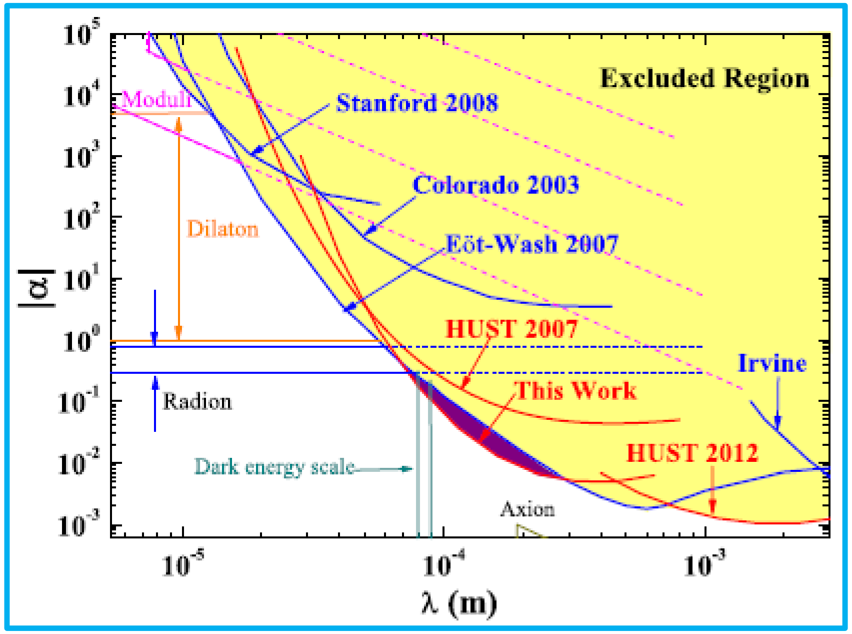

III. Experiments test for LV (d=6)

Potential between two point masses

$$V_{LV}(r) \equiv -G\frac{m_1 m_2}{r^3}\bar{k}(\hat{r}) \qquad r = \left|\vec{x}_1 - \vec{x}_2\right|$$

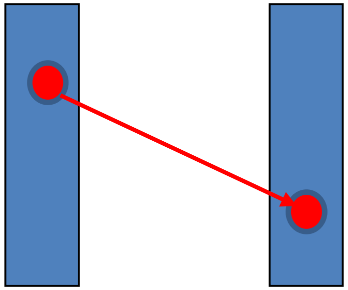

$$\bar{k}(\hat{r}) = \frac{3}{2}(\bar{k}_{eff})_{iijj} - 9(\bar{k}_{eff})_{ijkk}\hat{r}^i\hat{r}^j + \frac{15}{2}(\bar{k}_{eff})_{ijkl}\hat{r}^i\hat{r}^j\hat{r}^k\hat{r}^l$$

Sidereal Time T-dependent

$$(\bar{k}_{eff})_{jklm} = R^{jJ}R^{kK}R^{lL}R^{mM}(\bar{k}_{eff})_{JKLM}$$

Laboratory frame

Sun-centered frame

χ: colatitude of the lab

$$\omega_\oplus \simeq 2\pi / 23\text{h}56\,\text{min}$$

Earth's sidereal Frequency

$$R^{jJ} = \begin{pmatrix} \cos\chi\cos\omega_\oplus T & \cos\chi\sin\omega_\oplus T & -\sin\chi \\ -\sin\omega_\oplus T & \cos\omega_\oplus T & 0 \\ \sin\chi\cos\omega_\oplus T & \sin\chi\sin\omega_\oplus T & \cos\chi \end{pmatrix}$$

In laboratory frame

$$\bar{k}(\hat{r},T) = c_0 + \sum_{m=1}^{4}\left(c_m\cos m\omega_\oplus T + s_m\sin m\omega_\oplus T\right)$$

up to and including the fourth harmonic

LV force between two plates

Planar geometry: to suppress the Newtonian background

However, it also suppresses the LV signal

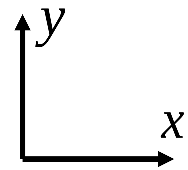

$$F^{y}_{Newton}(d)\Big|_{\text{infinite}} = \text{constant}$$

$$F^{y}_{LV}(d)\Big|_{\text{infinite}} = 0$$

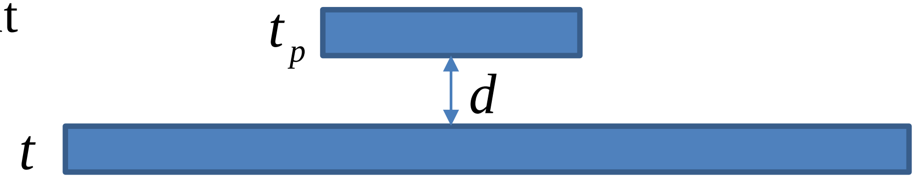

Force between two finite plates is dominated by the edge effect.

$$\Delta F^{y}_{LV} = F^{y}_{LV}(d_{\min}) - F^{y}_{LV}(d_{\max}) \sim \varepsilon\, \Delta C(\overline{k}_{eff})_{jkjk}$$

HUST-2011

$$\Delta C \equiv 2\pi G \rho_p \rho A_p \left[\ln \frac{(d_{\min}+t_p)(d_{\min}+t)}{(d_{\min}+t_p+t)d_{\min}} - \ln \frac{(d_{\max}+t_p)(d_{\max}+t)}{(d_{\max}+t_p+t)d_{\max}} \right]$$

dimensionless parameter ε： edge effect

Edge effect ε is typically of order ~0.01 or $d/\sqrt{A}$

Experimental result of LV for HUST-2011

$\tau^{z}_{measured}(t) = \tau_{LV}(T)\cos(2\pi f_s t + \varphi)$ LV torque was modulated by changing d

$$\tau_{LV}(T) = C_0 + \sum_{m=1}^{4}\left[C_m \cos(m\omega_{\oplus}T) + S_m \sin(m\omega_{\oplus}T)\right]$$

	10^{-16}Nm
C_0	-0.22±0.95
C_1	0.13±0.22
S_1	-0.40±0.23
C_2	-0.04±0.22
S_2	0.20±0.22
C_3	-0.30±0.22
S_3	-0.25±0.23
C_4	-0.06±0.23
S_4	0.05±0.23

	Keff	10^{-8}m^2
1	XXXX	-0.2±2.8
2	YYYY	0.4±2.8
3	ZZZZ	-0.9±7.7
4	XXXY	0.4±1.3
5	XXXZ	-0.1±0.5
6	YYYX	0.6±1.3
7	YYYZ	-0.4±0.5
8	ZZZX	-1.3±1.4
9	ZZZY	-0.2±1.3
10	XXYY	-0.1±1.7
11	XXZZ	-0.2±1.0
12	YYZZ	0.2±1.0
13	XXYZ	0.5±0.5
14	YYXZ	-0.2±0.5
15	ZZXY	-0.2±0.5

16×16×1.8 mm³

21×21×1.8 mm³

Area

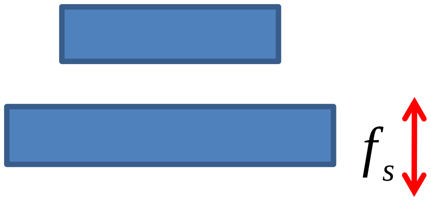

C.G. Shao,et.al.
PRD91, 102007 (2015)

Each constraint of $(\overline{k}_{eff})_{JKLM}$ was obtained in turn by setting the other 14 degrees of freedom to be zero.

J.C. Long,et.al.
PRD91, 092003 (2015)

Our result: similar to that of IU-2002,2012, a shorter range ISL experiment (80μm)

The LV constraint from combined analysis

HUST-2015 separation: 0.295 mm

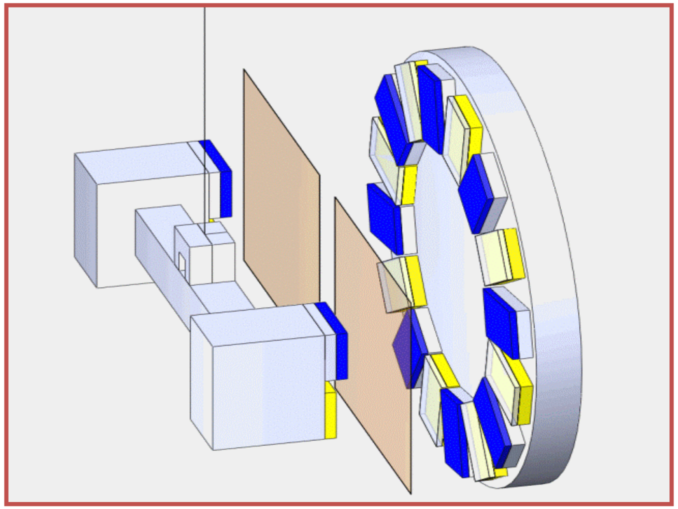

IU-2002,2012

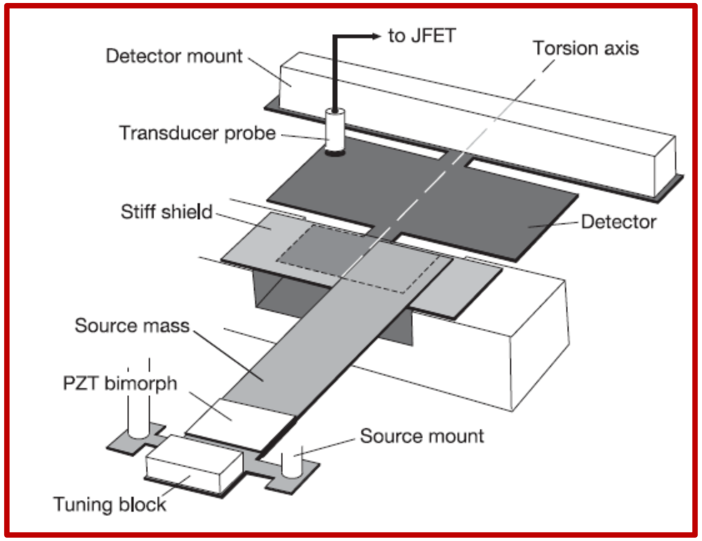

Combined analysis for HUST-2015, HUST-2011, IU-2012, IU-2002

TABLE II. Independent coefficient values (2σ, units 10^{-9} m^2) obtained by combining HUST and IU data [8–10].

Coefficient	Measurement
$(\bar{k}_{\mathrm{eff}})_{XXXX}$	6.4 ± 32.9
$(\bar{k}_{\mathrm{eff}})_{XXXY}$	0.0 ± 8.1
$(\bar{k}_{\mathrm{eff}})_{XXXZ}$	-2.0 ± 2.6
$(\bar{k}_{\mathrm{eff}})_{XXYY}$	-0.9 ± 10.9
$(\bar{k}_{\mathrm{eff}})_{XXYZ}$	1.1 ± 1.2
$(\bar{k}_{\mathrm{eff}})_{XXZZ}$	-2.6 ± 17.1
$(\bar{k}_{\mathrm{eff}})_{XYYY}$	3.9 ± 8.1
$(\bar{k}_{\mathrm{eff}})_{XYYZ}$	-0.6 ± 1.2
$(\bar{k}_{\mathrm{eff}})_{XYZZ}$	-1.0 ± 1.0
$(\bar{k}_{\mathrm{eff}})_{XZZZ}$	-8.1 ± 10.3
$(\bar{k}_{\mathrm{eff}})_{YYYY}$	7.0 ± 32.9
$(\bar{k}_{\mathrm{eff}})_{YYYZ}$	0.3 ± 2.6
$(\bar{k}_{\mathrm{eff}})_{YYZZ}$	-2.5 ± 17.1
$(\bar{k}_{\mathrm{eff}})_{YZZZ}$	3.6 ± 10.2

Shao et.al, PRL117,071102(2016)

A spherical decomposition

A convenient formalism for analyzing short-range test of LV

Lagrange density $$L = L_0 + L_{LV} = L_0 + \frac{1}{4} h_{\mu\nu} (\hat{s}^{\mu\rho\nu\sigma} + \hat{q}^{\mu\rho\nu\sigma} + \hat{k}^{\mu\nu\rho\sigma}) h_{\rho\sigma}$$

V. A. Kostelecky. et al, PLB766,137-143(2017)

Cartesian coordinate system ⟺ spherical coordinate system

$$\bar{k}(\hat{r}, \mathrm{T}) = \sum_{jm} Y_{jm}(\theta, \phi)\, k_{jm}^{N(d)lab}$$ ⇒ **Lorentz violation coefficients**

$$k_{jm}^{N(d)lab} = \sum_{m'} e^{im\varphi} e^{im'\omega_{\oplus}T} d_{mm'}^{(j)}(-\chi) k_{jm'}^{N(d)}$$

$$\left\{ \begin{array}{l} j = d-2 \ or \ d-4 \\ m = -j, \cdots j \end{array} \right. \Rightarrow \left\{ \begin{array}{l} \mathrm{Re}\, k_{jm}^{N(d)} \\ \mathrm{Im}\, k_{jm}^{N(d)} \end{array} \right.$$

Lab frame

Sun-centered frame

The spherical decomposition provides a clean separation of the observable harmonics in sidereal time.

Transformation matrix(d=6)

Newton spherical coefficients ⟺ Effective Cartesian coefficients

$$
\begin{bmatrix} k_{2,0} \\ \mathrm{Re}\,k_{2,1} \\ \mathrm{Im}\,k_{2,-1} \\ \mathrm{Re}\,k_{2,2} \\ \mathrm{Im}\,k_{2,-2} \\ k_{4,0} \\ \mathrm{Re}\,k_{4,1} \\ \mathrm{Im}\,k_{4,-1} \\ \mathrm{Re}\,k_{4,2} \\ \mathrm{Im}\,k_{4,-2} \\ \mathrm{Re}\,k_{4,3} \\ \mathrm{Im}\,k_{4,-3} \\ \mathrm{Re}\,k_{4,4} \\ \mathrm{Im}\,k_{4,-4} \end{bmatrix}
= \frac{\sqrt{\pi}}{7}
\begin{bmatrix}
36/\sqrt{5} & 0 & 0 & 72/\sqrt{5} & 0 & 36/\sqrt{5} & 0 & 0 & 0 & 0 & 36/\sqrt{5} & 0 & 36/\sqrt{5} & 0 \\
0 & 0 & 12\sqrt{6/5} & 0 & 0 & 0 & 0 & 12\sqrt{6/5} & 0 & 12\sqrt{6/5} & 0 & 0 & 0 & 0 \\
0 & 0 & 0 & 0 & -12\sqrt{6/5} & 0 & 0 & 0 & 0 & 0 & 0 & -12\sqrt{6/5} & 0 & -12\sqrt{6/5} \\
-6\sqrt{6/5} & 0 & 0 & 0 & 0 & 6\sqrt{6/5} & 0 & 0 & 0 & 0 & 6\sqrt{6/5} & 0 & 6\sqrt{6/5} & 0 \\
0 & 12\sqrt{6/5} & 0 & 0 & 0 & 0 & 12\sqrt{6/5} & 0 & 12\sqrt{6/5} & 0 & 0 & 0 & 0 & 0 \\
-5 & 0 & 0 & -10 & 0 & -40\sqrt{10} & 0 & 0 & 0 & 0 & -5 & 0 & -40 & 0 \\
0 & 0 & 6 & 0 & 0 & 0 & 0 & 6\sqrt{5} & 0 & -8\sqrt{5} & 0 & 0 & 0 & 0 \\
0 & 0 & 0 & 0 & -6\sqrt{5} & 0 & 0 & 0 & 0 & 0 & 0 & -6\sqrt{5} & 0 & 8\sqrt{5} \\
-\sqrt{10} & 0 & 0 & 0 & 0 & -10\sqrt{5} & 0 & 0 & 0 & 0 & \sqrt{10} & 0 & -6\sqrt{10} & 0 \\
0 & 2\sqrt{10} & 0 & 0 & 0 & 0 & 2\sqrt{10} & 0 & -12\sqrt{10} & 0 & 0 & 0 & 0 & 0 \\
0 & 0 & -2\sqrt{35} & 0 & 0 & 0 & 0 & 6\sqrt{35} & 0 & 0 & 0 & 0 & 0 & 0 \\
0 & 0 & 0 & 0 & 6\sqrt{35} & 0 & 0 & 0 & 0 & 0 & 0 & -2\sqrt{35} & 0 & 0 \\
\sqrt{5/2} & 0 & 0 & -3\sqrt{70} & 0 & 0 & 0 & 0 & 0 & 0 & \sqrt{5/2} & 0 & 0 & 0 \\
0 & -2\sqrt{70} & 0 & 0 & 0 & 0 & 2\sqrt{70} & 0 & 0 & 0 & 0 & 0 & 0 & 0
\end{bmatrix}
\begin{bmatrix} (\bar{k}_{eff})_{XXXX} \\ (\bar{k}_{eff})_{XXXY} \\ (\bar{k}_{eff})_{XXXZ} \\ (\bar{k}_{eff})_{XXYY} \\ (\bar{k}_{eff})_{XXYZ} \\ (\bar{k}_{eff})_{XXZZ} \\ (\bar{k}_{eff})_{XYYY} \\ (\bar{k}_{eff})_{XYYZ} \\ (\bar{k}_{eff})_{XYZZ} \\ (\bar{k}_{eff})_{XZZZ} \\ (\bar{k}_{eff})_{YYYY} \\ (\bar{k}_{eff})_{YYYZ} \\ (\bar{k}_{eff})_{YYZZ} \\ (\bar{k}_{eff})_{YZZZ} \end{bmatrix}
$$

V. A. Kostelecky. Et al, PLB766,137-143(2017)

Result for spherical coefficients

Cartesian Coefficients

Coefficient	Measurement
$(\bar{k}_{\text{eff}})_{XXXX}$	6.4 ± 32.9
$(\bar{k}_{\text{eff}})_{XXXY}$	0.0 ± 8.1
$(\bar{k}_{\text{eff}})_{XXXZ}$	-2.0 ± 2.6
$(\bar{k}_{\text{eff}})_{XXYY}$	-0.9 ± 10.9
$(\bar{k}_{\text{eff}})_{XXYZ}$	1.1 ± 1.2
$(\bar{k}_{\text{eff}})_{XXZZ}$	-2.6 ± 17.1
$(\bar{k}_{\text{eff}})_{XYYY}$	3.9 ± 8.1
$(\bar{k}_{\text{eff}})_{XYYZ}$	-0.6 ± 1.2
$(\bar{k}_{\text{eff}})_{XYZZ}$	-1.0 ± 1.0
$(\bar{k}_{\text{eff}})_{XZZZ}$	-8.1 ± 10.3
$(\bar{k}_{\text{eff}})_{YYYY}$	7.0 ± 32.9
$(\bar{k}_{\text{eff}})_{YYYZ}$	0.3 ± 2.6
$(\bar{k}_{\text{eff}})_{YYZZ}$	-2.5 ± 17.1
$(\bar{k}_{\text{eff}})_{YZZZ}$	3.6 ± 10.2

Derived values of Newton spherical coefficients.

Coefficient	Measurement
$k_{20}^{\mathrm{N}(6)}$	$(3 \pm 23) \times 10^{-8}\ \mathrm{m}^2$
Re $k_{21}^{\mathrm{N}(6)}$	$(-4 \pm 4) \times 10^{-8}\ \mathrm{m}^2$
Im $k_{21}^{\mathrm{N}(6)}$	$(-2 \pm 4) \times 10^{-8}\ \mathrm{m}^2$
Re $k_{22}^{\mathrm{N}(6)}$	$(0 \pm 9) \times 10^{-8}\ \mathrm{m}^2$
Im $k_{22}^{\mathrm{N}(6)}$	$(1 \pm 4) \times 10^{-8}\ \mathrm{m}^2$
$k_{40}^{\mathrm{N}(6)}$	$(4 \pm 25) \times 10^{-8}\ \mathrm{m}^2$
Re $k_{41}^{\mathrm{N}(6)}$	$(3 \pm 5) \times 10^{-8}\ \mathrm{m}^2$
Im $k_{41}^{\mathrm{N}(6)}$	$(1 \pm 5) \times 10^{-8}\ \mathrm{m}^2$
Re $k_{42}^{\mathrm{N}(6)}$	$(0 \pm 12) \times 10^{-8}\ \mathrm{m}^2$
Im $k_{42}^{\mathrm{N}(6)}$	$(2 \pm 2) \times 10^{-8}\ \mathrm{m}^2$
Re $k_{43}^{\mathrm{N}(6)}$	$(0 \pm 1) \times 10^{-8}\ \mathrm{m}^2$
Im $k_{43}^{\mathrm{N}(6)}$	$(1 \pm 1) \times 10^{-8}\ \mathrm{m}^2$
Re $k_{44}^{\mathrm{N}(6)}$	$(2 \pm 9) \times 10^{-8}\ \mathrm{m}^2$
Im $k_{44}^{\mathrm{N}(6)}$	$(2 \pm 5) \times 10^{-8}\ \mathrm{m}^2$

C. G. Shao. Et al, PRL117,071102(2016)   V. A. Kostelecky. Et al, PLB766,137-143(2017)

IV. New experimental design for LV(d=6)

- Almost all experiments on ISL adopt planar geometry to search for Yukawa-type non-Newton gravity, which also suppressed LV signal

- LV force between two finite flat plates is dominated by edge effect

To increase the signal of LV

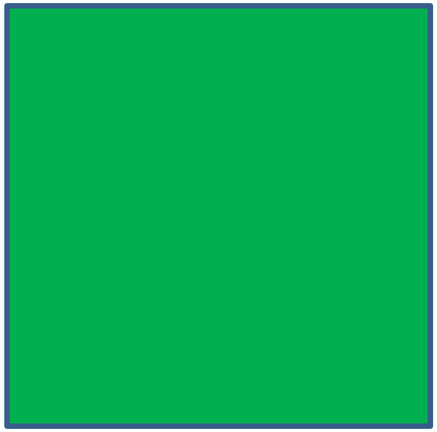

homogeneous-plate

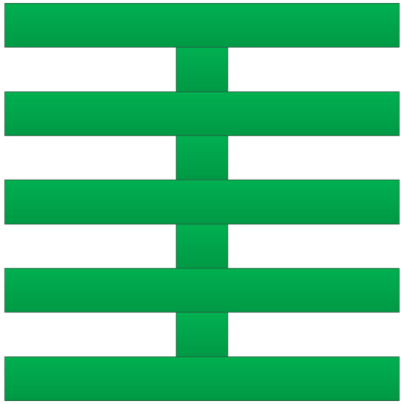

striped pattern

14 measurable independently coefficients of LV

Double trace of $(\bar{k}_{eff})_{ijij}$ is a rotational scalar, and can't be measured in short-range gravity

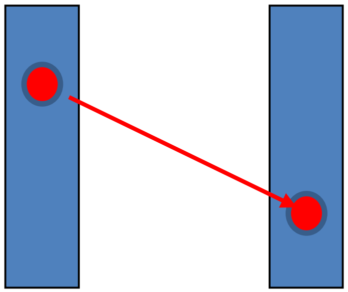

Measured LV torque provides nine components

$$\tau_{LV} = C_0 + \sum_{m=1}^{4} C_m \cos(m\omega_{\oplus} T) + S_m \sin(m\omega_{\oplus} T)$$

Equivalently, $\bar{k}(\hat{r}) = c_0 + \sum_{m=1}^{4} c_m \cos(m\omega_{\oplus} T) + s_m \sin(m\omega_{\oplus} T)$

Nine components in $\bar{k}(\hat{r})$ are functions of the 14 constant coefficients $(\bar{k}_{eff})$ in Sun-centered frame.

14 measurable coefficients in spherical coordinate system provides a clean separation of the observable harmonics.

$C_i,\ S_i \leftrightarrow k_{jm}$ through functions 14 $\Gamma_j(\theta,\chi)$

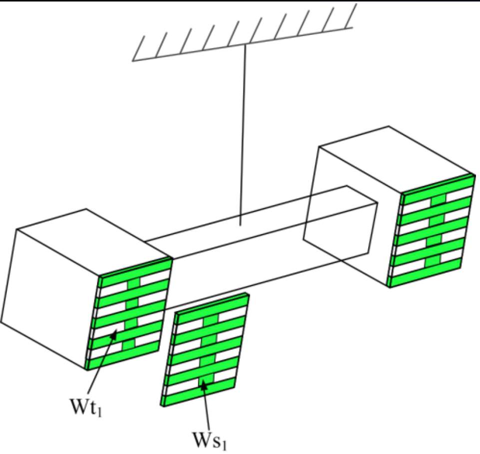

Test mass element: $dm_1 = \rho_1 dV_1$

Source mass element: $dm_2 = \rho_2 dV_2$

$$\tau_{\mathrm{LV}}(T) = C_0 + \sum_{m=1}^{4}\left(C_m \cos m\omega_{\oplus}T + S_m \sin m\omega_{\oplus}T\right)$$

$$\begin{bmatrix} C_0 \\ C_2 \\ S_2 \\ C_4 \\ S_4 \\ C_1 \\ S_1 \\ C_3 \\ S_3 \end{bmatrix} = \begin{bmatrix} \Gamma_1 & \Gamma_2 & 0 & 0 & 0 & 0 & 0 & 0 & 0 & 0 & 0 & 0 & 0 & 0 \\ 0 & 0 & \Gamma_3 & \Gamma_4 & \Gamma_5 & \Gamma_6 & 0 & 0 & 0 & 0 & 0 & 0 & 0 & 0 \\ 0 & 0 & \Gamma_4 & -\Gamma_3 & \Gamma_6 & -\Gamma_5 & 0 & 0 & 0 & 0 & 0 & 0 & 0 & 0 \\ 0 & 0 & 0 & 0 & 0 & 0 & \Gamma_7 & \Gamma_8 & 0 & 0 & 0 & 0 & 0 & 0 \\ 0 & 0 & 0 & 0 & 0 & 0 & \Gamma_8 & -\Gamma_7 & 0 & 0 & 0 & 0 & 0 & 0 \\ 0 & 0 & 0 & 0 & 0 & 0 & 0 & 0 & \Gamma_9 & \Gamma_{10} & \Gamma_{11} & \Gamma_{12} & 0 & 0 \\ 0 & 0 & 0 & 0 & 0 & 0 & 0 & 0 & \Gamma_{10} & -\Gamma_9 & \Gamma_{12} & -\Gamma_{11} & 0 & 0 \\ 0 & 0 & 0 & 0 & 0 & 0 & 0 & 0 & 0 & 0 & 0 & 0 & \Gamma_{13} & \Gamma_{14} \\ 0 & 0 & 0 & 0 & 0 & 0 & 0 & 0 & 0 & 0 & 0 & 0 & \Gamma_{14} & -\Gamma_{13} \end{bmatrix} \begin{bmatrix} k_{2,0} \\ k_{4,0} \\ \mathrm{Re}\,k_{2,2} \\ \mathrm{Im}\,k_{2,2} \\ \mathrm{Re}\,k_{4,2} \\ \mathrm{Im}\,k_{4,2} \\ \mathrm{Re}\,k_{4,4} \\ \mathrm{Im}\,k_{4,4} \\ \mathrm{Re}\,k_{2,1} \\ \mathrm{Im}\,k_{2,1} \\ \mathrm{Re}\,k_{4,1} \\ \mathrm{Im}\,k_{4,1} \\ \mathrm{Re}\,k_{4,3} \\ \mathrm{Im}\,k_{4,3} \end{bmatrix}$$

Any experimental design should make Γ_j as large as possible.

Schematic drawing

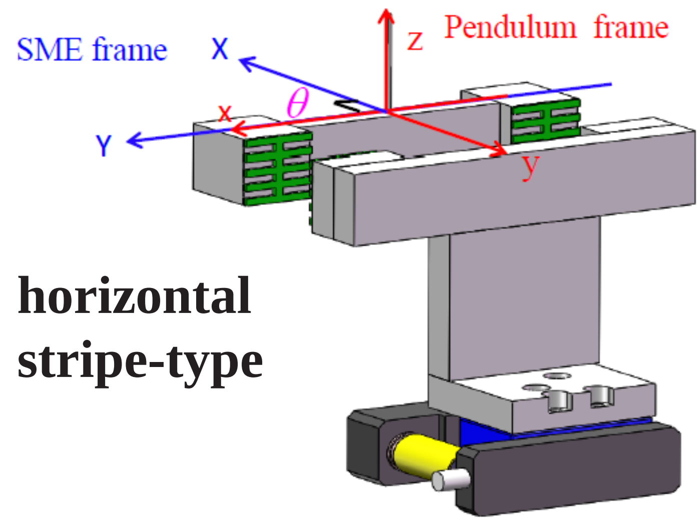

horizontal stripe-type

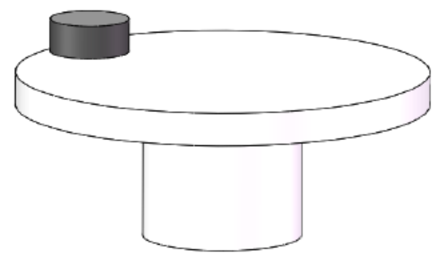

a)

Each strip:

1.3×19.8×2.2 mm^3

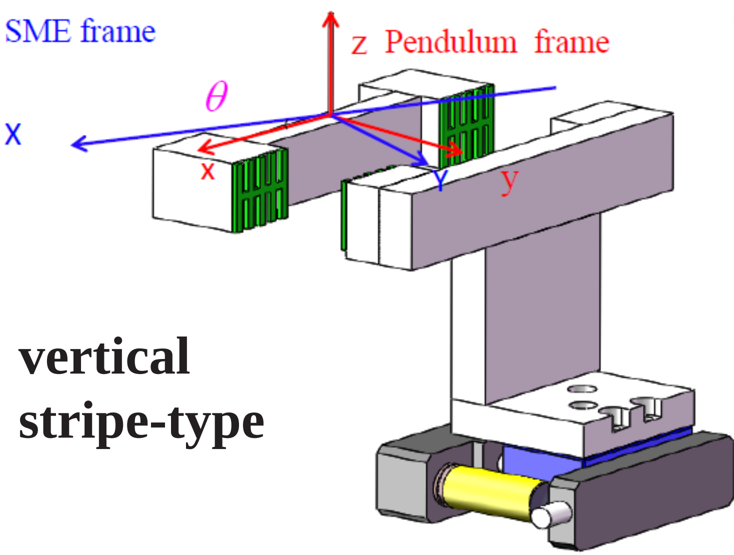

vertical stripe-type

motor translation stage:

gap varies from 0.4 to 1 mm

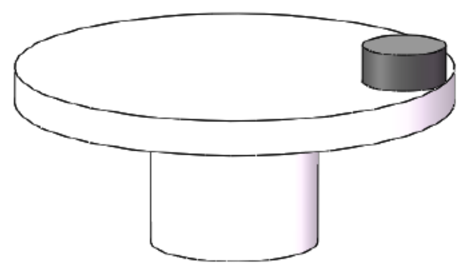

b)

The feature for test and source masses

Set horizontal stripe as an example

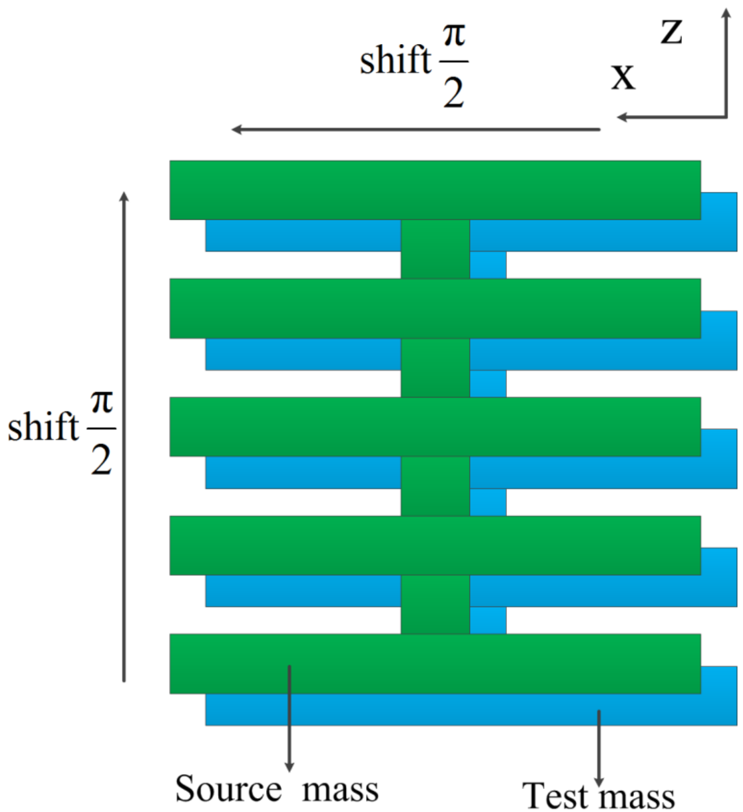

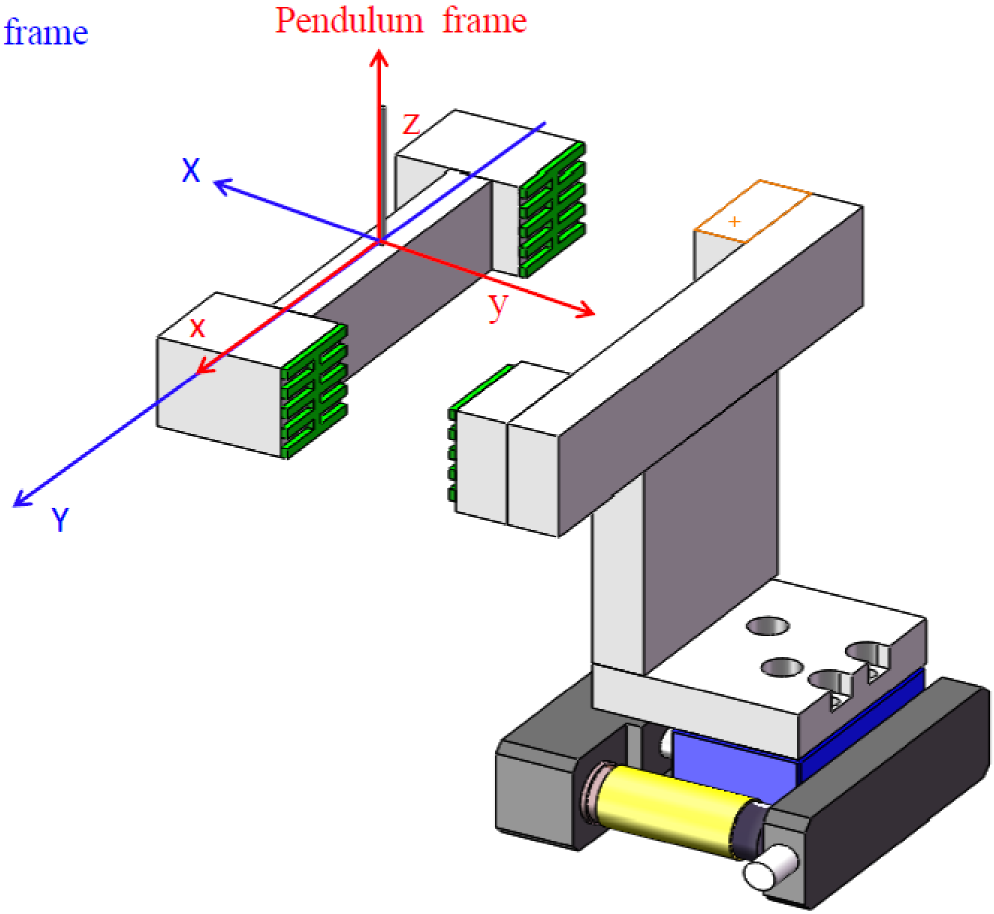

shifted up and left half of the width of the strip

Transfer coefficients vary with angle

According to the typical design parameters， we calculate transfer coefficients as functions of angle

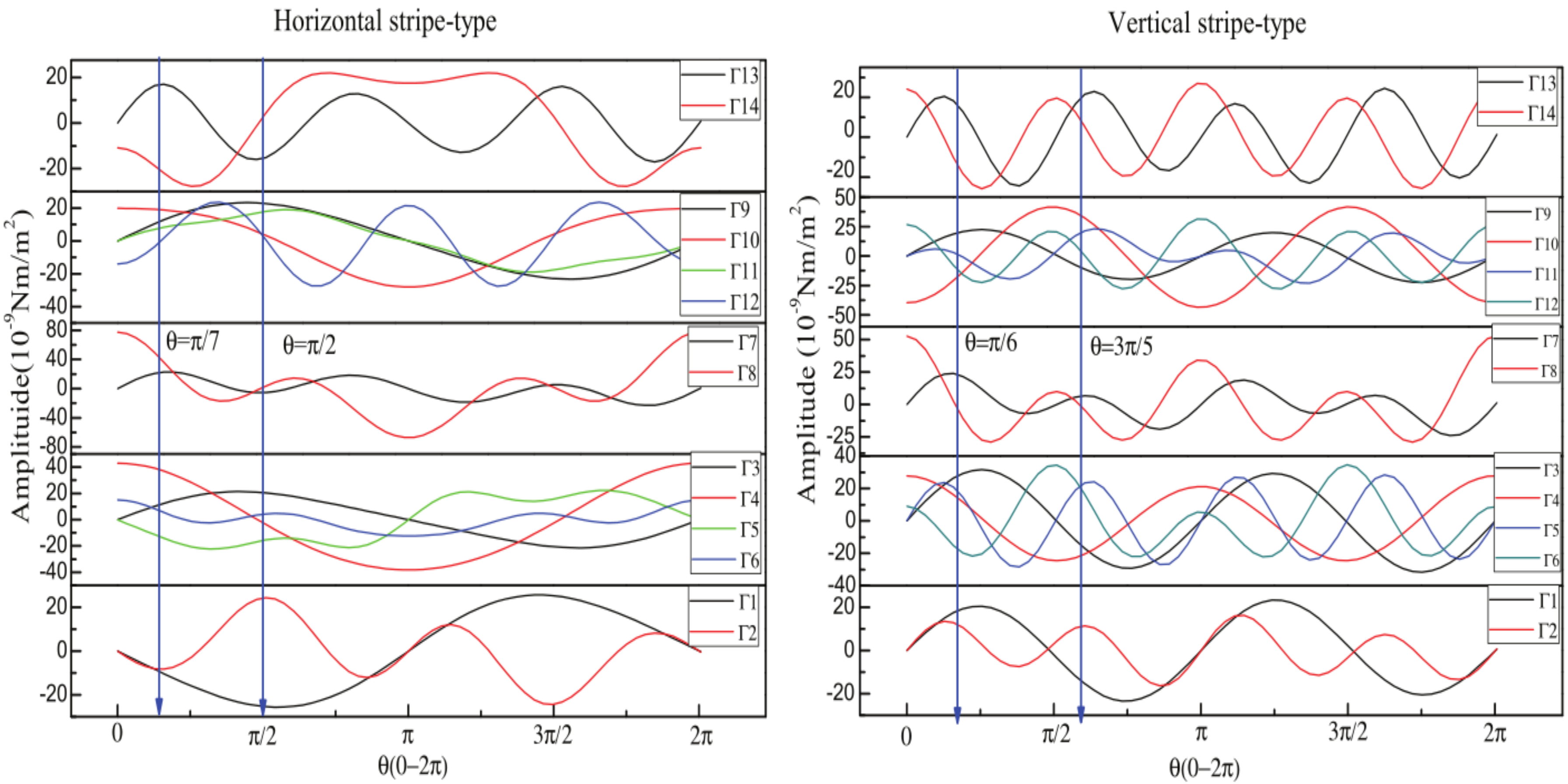

Symmetry 9, 219 (2017)

Expected signal

Compare to the best current constraint[1]

Assuming 3 μm systemic error

Ratio of the total error in the current best constraint to that in our new design

Coefficients	Current constraint (10^{-8}m^2)[21]	Ratio in horizontal stripe-type for $\theta = \pi/7$ and $\pi/2$	Ratio in vertical stripe-type for $\theta = \pi/6$ and $3\pi/5$
$k_{2,0}$	3 ± 23	4	5
$\mathrm{Re}\, k_{1,1}$	-4 ± 4	16	21
$\mathrm{Im}\, k_{2,1}$	-2 ± 4	16	21
$\mathrm{Re}\, k_{2,2}$	0 ± 9	67	73
$\mathrm{Im}\, k_{2,2}$	1 ± 4	30	32
$k_{4,0}$	4 ± 25	4	4
$\mathrm{Re}\, k_{4,1}$	3 ± 5	13	14
$\mathrm{Im}\, k_{4,1}$	1 ± 5	13	14
$\mathrm{Re}\, k_{2,2}$	0 ± 12	44	92
$\mathrm{Im}\, k_{2,2}$	2 ± 2	7	15
$\mathrm{Re}\, k_{4,3}$	0 ± 1	7	7
$\mathrm{Im}\, k_{4,3}$	1 ± 1	7	7
$\mathrm{Re}\, k_{4,4}$	2 ± 9	97	49
$\mathrm{Im}\, k_{4,4}$	2 ± 5	54	27

[1] V. A. Kostelecky. Et al, PLB766,137-143(2017)

Experimental process

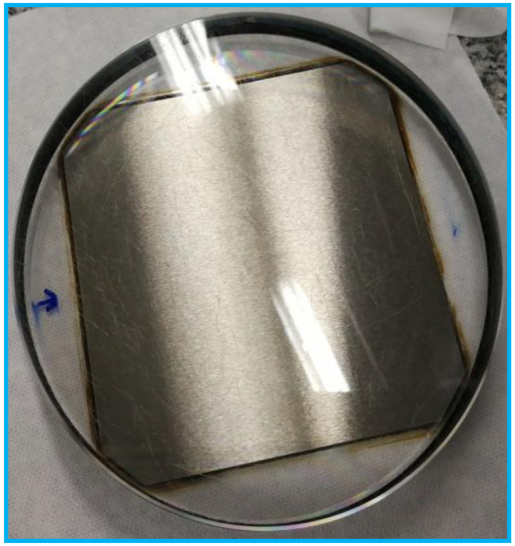

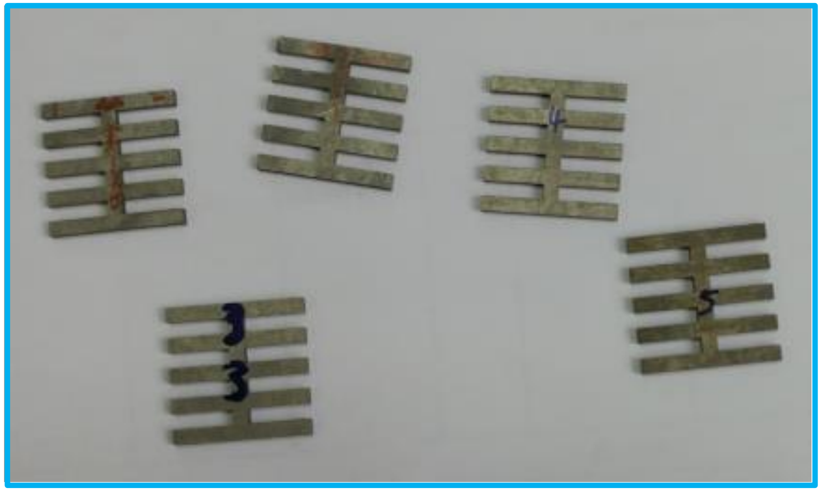

The experiment is ongoing

Conclusion and prospect

Conclusion

- For Quadratic couplings of Riemann curvature with d=6, the ISL experiments can be used to constrain the LV
- We suggested experiments with periodic striped geometry, which may improve the current constraints of LV by about one order of magnitude and the experiment is ongoing.

Prospect

- The ISL experiments and new design experiments may also be used to test LV effect for d=8, which is now being under study.